

Cite this: *Chem. Sci.*, 2022, **13**, 6254

All publication charges for this article have been paid for by the Royal Society of Chemistry

Received 28th March 2022

Accepted 4th May 2022

DOI: 10.1039/d2sc01782b

rsc.li/chemical-science

## Cagearenes: synthesis, characterization, and application for programmed vapour release†

Shuai Fang,<sup>a</sup> Mengbin Wang,<sup>a</sup> Yating Wu,<sup>b</sup> Qing-Hui Guo,<sup>bc</sup> Errui Li,<sup>\*a</sup> Hao Li<sup>Id</sup> <sup>\*bc</sup> and Feihe Huang <sup>ID</sup> <sup>\*ac</sup>

Here, we announce the establishment of a new family of organic molecular cages, named cagearenes, by taking advantage of a versatile strategy. These cagearenes were prepared *via* the Friedel–Crafts reaction by condensing two equivalents of a precursor bearing three 1,4-dimethoxybenzene groups and three equivalents of formaldehyde. Two cages, namely **cagearene-1** and **cagearene-2**, are obtained and well characterized. The **cagearene-1** solid exhibits the ability to adsorb benzene vapour from an equimolar benzene/cyclohexane mixture with a purity of 91.1%. Then, the adsorbed benzene molecules can be released from the cage at a relatively lower temperature, namely 70 °C, as a consequence of which, cyclohexane with a high purity was left within the cage solid. Heating the cage solid further at 130 °C led to the production of cyclohexane with a purity up to 98.7%. As inferred from the single crystal structures and theoretical calculations, the ability of the cage in programmed release of benzene and cyclohexane results from the different binding modes of these two guests.

## Introduction

Programmed release is of great significance in both biomedical and chemical production, especially in drug delivery and adsorption/separation applications.<sup>1</sup> Different targets can be released procedurally under different environmental stimuli (such as electric or magnetic fields,<sup>2</sup> enzymes,<sup>3</sup> temperature,<sup>4</sup> etc.) to achieve the desired functions. Specifically, in the field of adsorption/separation, it is desired that different hydrocarbon compounds can be released stepwise and obtained in high purities in one absorption/desorption cycle by taking advantage of programmed release. This is economical and meaningful in industrial separation, because it can replace many tedious separation processes and greatly reduce energy consumption. Therefore, it is necessary to seek and synthesize suitable materials or compounds to achieve such programmed release. In the past decade, programmed release has been explored in the chemistry of extended frameworks, such as metal–organic frameworks (MOFs).<sup>5</sup> The pores in these materials were chemically and geometrically designed to efficiently and selectively

bind a single guest molecule. Although host–guest interactions in these materials have been studied, the ability to create a desired environment and thus realize precisely programmed release of different hydrocarbon compounds is very challenging and remains largely undeveloped.

Supramolecular hosts may be good candidates for programmed release, in the case that the hosts have a high absorption affinity to hydrocarbon compounds and rich environmental responsiveness based on host–guest interactions.<sup>6</sup> Under external stimuli, the programmed release of hydrocarbons may be realized because guest accommodation might occur in different modes. However, in the case of a macrocyclic host, host–guest recognition often occurs in the cavity of the macrocycle. As a consequence, different guests might experience similar chemical environments and therefore undergo similar host–guest interactions. Such behavior leads to difficulty in programmed release of different guests. The question of concern here is whether programmed release can be achieved by creating a new cavity environment, such as the cavity of an organic cage, where one host accommodates different guest molecules *via* different interacting modes.

The interest in organic cage compounds, extended from macrocycles, is nearly as old as the interest in supramolecular chemistry.<sup>7</sup> Organic cages have been applied in host–guest chemistry,<sup>8</sup> aromatic systems,<sup>9</sup> separation,<sup>10</sup> catalysis,<sup>11</sup> and assembly.<sup>12</sup> Until now, a variety of synthetic strategies have been employed to access organic cages. Among these, the use of reversible bond formation, or dynamic covalent chemistry (DCC), is the most common method, which has some advantages in terms of high yield and the ability to form self-

<sup>a</sup>Department of Chemistry, State Key Laboratory of Chemical Engineering, Stoddart Institute of Molecular Science, Zhejiang University, Hangzhou 310027, P. R. China. E-mail: fhuang@zju.edu.cn; erruili@zju.edu.cn; Fax: +86 571 87953189

<sup>b</sup>Department of Chemistry, Stoddart Institute of Molecular Science, Zhejiang University, Hangzhou 310027, P. R. China. E-mail: lihao2015@zju.edu.cn

<sup>c</sup>ZJU-Hangzhou Global Scientific and Technological Innovation Center, Hangzhou 311215, P. R. China

† Electronic supplementary information (ESI) available. CCDC 2116328–2116331. For ESI and crystallographic data in CIF or other electronic format see <https://doi.org/10.1039/d2sc01782b>



assembled cages in a one-pot manner.<sup>13</sup> However, the relatively labile bonds from DCC reactions often result in poor structural and chemical stability, and it is difficult for further synthetic modification. Irreversible chemical bonds as an alternative strategy have also been applied to construct cages, although few.<sup>14</sup> Very recently, Li's group ingeniously developed a one-pot, shape-controlled synthesis of two covalent organic cages *via* the Friedel-Crafts (FC) reaction.<sup>15</sup> However, the poor solubility of the bigger cage and the narrow cavity of the smaller cage prevented further research in programmed release based on host-guest interactions.

Here, we present the syntheses of two new organic cages and their application in programmed release. Precursors composed of 1,4-dimethoxybenzene groups were first synthesized, and then *para*-bridged by methylenes to obtain **cagearene-1** and **cagearene-2**. For **cagearene-1**, we tested its absorption and separation ability in the solid state. It was found that **cagearene-1** could adsorb benzene from an equimolar benzene/cyclohexane mixture (50 : 50 v/v) with a purity of 91.1%. More interestingly, benzene and cyclohexane could be both obtained with high purities in one absorption/desorption cycle due to their different release temperatures. We attributed this phenomenon to the different host-guest interactions between different guest molecules and the cage, which is supported by single crystal X-ray and computational analyses.

## Results and discussion

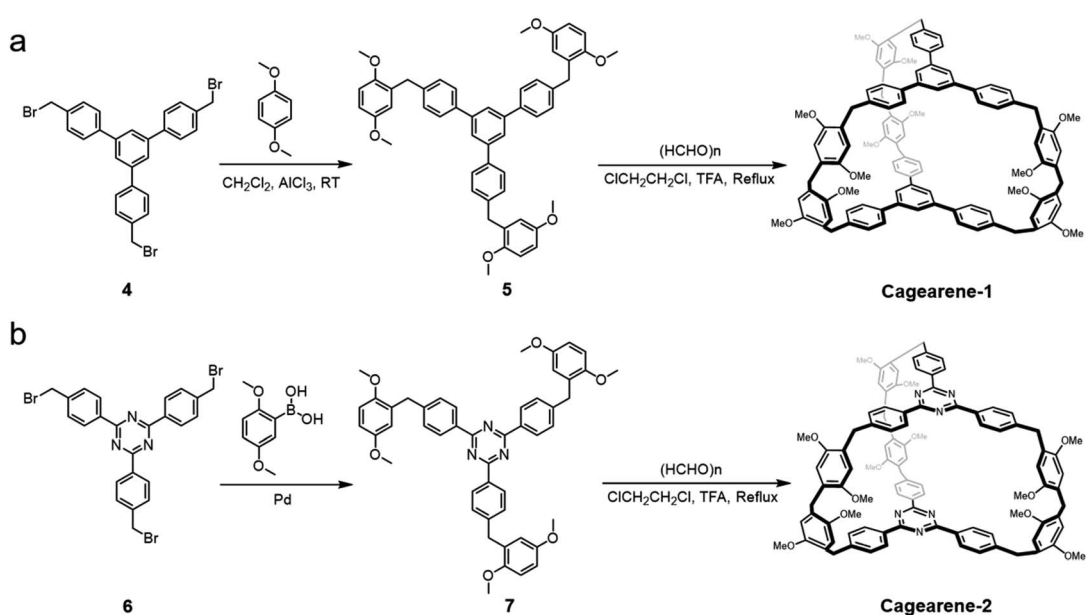
### Synthesis of cagearenes

Cagearenes are defined as three dimensional organic cages in which aromatic units are connected by methylene groups. Our design of these FC-based cagearenes is shown in Scheme 1. Here, two new organic cages, **cagearene-1** and **cagearene-2**, were prepared, for both of which three lateral edges link two

aromatic building blocks. Each lateral edge contains two 1,4-dimethoxybenzene groups which are bridged by one methylene group.

The key step in the syntheses of these two cagearenes is the initial formation of the precursors. In detail, precursor **5** was prepared first by combining 1,3,5-tris(*p*-bromomethylphenyl)benzene and 1,4-dimethoxybenzene in the presence of aluminum chloride ( $\text{AlCl}_3$ ) in 46% yield (Scheme 1a). Then, by mixing **5** with an excess of paraformaldehyde, **cagearene-1** was synthesized *via* cyclization in a [2 + 3] manner. Several trials were performed to obtain the optimal reaction conditions. As shown in Table S1,<sup>†</sup> a high temperature was crucial and mandatory for cage formation. Various catalysts, such as  $\text{CF}_3\text{COOH}$  (TFA),  $\text{BF}_3\text{:OEt}_2$ ,  $\text{CF}_3\text{SO}_3\text{H}$ , *p*-toluenesulfonic acid and  $\text{AlCl}_3$ , were all tested, and TFA showed the best catalytic performance. Besides, humidity, especially a high humidity environment, had negative effects on the reaction yields. Under optimized conditions, the reaction gave only one major product, **cagearene-1**, in 31% yield.

The possibility of using the developed strategy to construct new cages was investigated by introducing new building blocks. We anticipated that replacing the 1,3,5-triphenylbenzene units with 2,4,6-triphenyl-1,3,5-triazine moieties would produce a similar cage, namely **cagearene-2** (Scheme 1b). However, the FC reaction between 2,4,6-tris(*p*-bromomethylphenyl)-1,3,5-triazine and 1,4-dimethoxybenzene did not occur under the catalysis of a Lewis acid. In order to get **cagearene-2**, precursor **7** was synthesized *via* a transition metal-catalyzed cross-coupling reaction to connect one 2,4,6-triphenyl-1,3,5-triazine unit and three 1,4-dimethoxybenzene units. Under the same optimal reaction condition as above, **cagearene-2** was obtained with 21% yield. The successful formation of **cagearene-1** and **cagearene-2** clearly verified that this strategy was a versatile one for forming diverse cages.



Scheme 1 Syntheses of (a) **cagearene-1** and (b) **cagearene-2**.



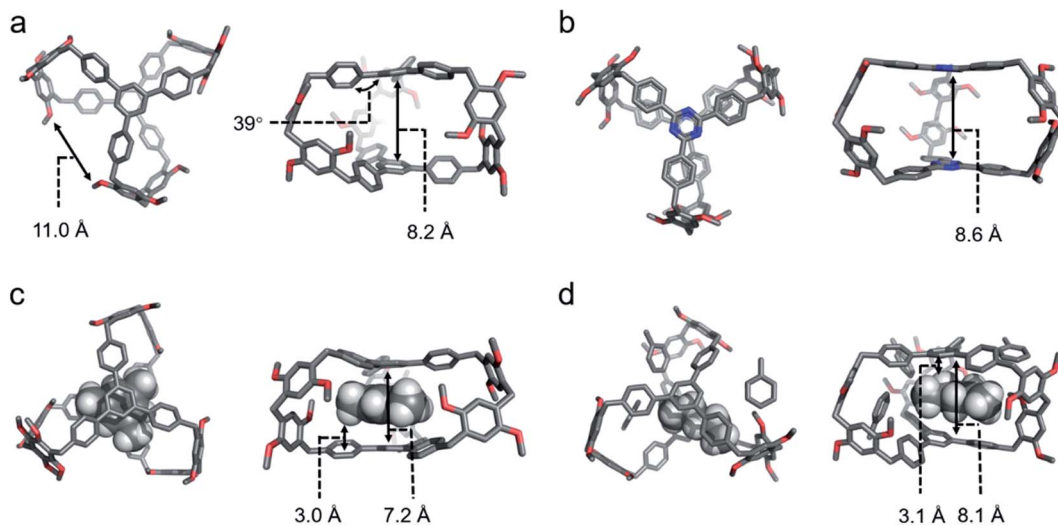


Fig. 1 Structures of (a) cagearene-1, (b) cagearene-2, (c) 1,3,5-trimethylbenzene@cagearene-1, and (d) pentane@cagearene-1 (top and side views). The structures of cagearene-1, 1,3,5-trimethylbenzene@cagearene-1, and pentane@cagearene-1 were obtained from single crystal X-ray diffraction analysis, while the structure of cagearene-2 was obtained from DFT calculations. Certain H atoms are omitted for clarity. The cages are illustrated in a stick representation, while the guest molecules are in a space-filling representation. Color code: C gray, N blue, O red, and H white.

## Characterization studies of cagearenes

The structure of **cagearene-1** was fully confirmed by nuclear magnetic resonance spectrometry ( $^1\text{H}$  NMR,  $^{13}\text{C}$  NMR, and 2D  $^1\text{H}$ - $^1\text{H}$  COSY) (Fig. S4–S7 $\dagger$ ), MS spectrometry (Fig. S8 $\dagger$ ) and X-ray single crystal diffraction (Fig. 1a). The corresponding  $^1\text{H}$  NMR spectrum of **cagearene-1** showed seven singlet signals and two doublet signals, corresponding to benzene ring protons H<sub>1</sub>, H<sub>2</sub>, H<sub>3</sub>, H<sub>4</sub> and H<sub>5</sub>, methylene protons H<sub>6</sub> and H<sub>7</sub>, and methyl protons H<sub>8</sub> and H<sub>9</sub>, which were also assigned by using 2D  $^1\text{H}$ - $^1\text{H}$  COSY and NOESY spectra (Fig. S4, S6 and S7 $\dagger$ ). Moreover, fifteen signals were observed in the  $^{13}\text{C}$  NMR spectrum (Fig. S5 $\dagger$ ). These results were consistent with the  $D_3$  symmetrical structure of **cagearene-1**.

A nitrogen sorption experiment at 77 K showed that **cagearene-1** was negligibly porous, with a BET surface area of 56  $\text{m}^2 \text{ g}^{-1}$  (Fig. S24 $\dagger$ ). Broadened signals were observed in the powder X-ray diffraction (PXRD) data of the activated **cagearene-1** (Fig. 2a), suggesting that the solid was in the amorphous state.

The crystal structure of **cagearene-1** confirmed that two 1,3,5-triphenylbenzene subunits grafted by six 1,4-dimethoxybenzene

were all connected by methylene groups at *para*-positions to form a cage-shaped structure (Fig. 1a). The average angle between the three side phenyl rings and the central phenyl panel in each 1,3,5-triphenylbenzene subunit is about 39°. The average distance between the “roof” and “floor” aromatic faces is 8.2 Å, and the average distance between two lateral edges is 11.0 Å, producing the intrinsic cavity of **cagearene-1**.

Identically, the structure of **cagearene-2** was also confirmed by  $^1\text{H}$  NMR,  $^{13}\text{C}$  NMR,  $^1\text{H}$ - $^1\text{H}$  COSY spectrometry (Fig. S12–S15 $\dagger$ ), and MS spectrometry (Fig. S16 $\dagger$ ). Numerous attempts to grow single crystals of **cagearene-2** under different conditions did not meet with success. Density functional theory (DFT) calculations at the B3LYP-D3/6-31G level were performed in order to generate the structure of **cagearene-2** (Fig. 1b). It revealed that the “roof” and “floor” of **cagearene-2** were planar, which was inherited from the 2,4,6-triphenyl-1,3,5-triazine unit.<sup>16</sup> Unfortunately, it was found that **cagearene-2** was not as stable as **cagearene-1** which may be due to the instability of the 1,3,5-triazine unit,<sup>17</sup> which obstructed its further use in the research of programmed release.

## Host–Guest complexes of cagearene-1 in the solid state

The cavity of **cagearene-1** indicated that it had a nearly perfect structure for encapsulating guest molecules. This speculation was unambiguously confirmed by the crystal structures of two inclusion complexes, 1,3,5-trimethylbenzene@cagearene-1 and pentane@cagearene-1 (Fig. 1c and d). Single crystals of 1,3,5-trimethylbenzene@cagearene-1 were obtained by slow evaporation of a 1,3,5-trimethylbenzene solution of **cagearene-1**, while single crystals of pentane@cagearene-1 were prepared by evaporating pentane into a toluene solution of **cagearene-1**. In both cases, close contact occurred between the guest molecules and the cage host, indicating the existence of [C–H $\cdots$  $\pi$ ] and/or

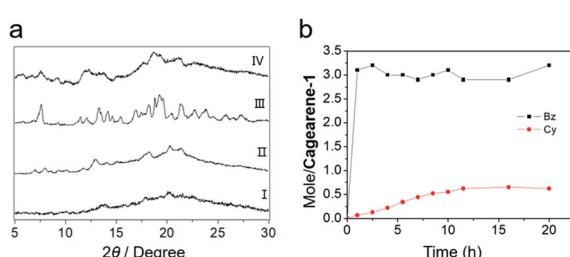


Fig. 2 (a) The PXRD patterns of cagearene-1: (I) original cagearene-1; (II) after adsorption of Cy vapour; (III) after adsorption of Bz vapour; (IV) after adsorption of Bz/Cy mixture vapour. (b) Time-dependent solid-vapour sorption plot for single-component Bz or Cy vapour.

$[\pi-\pi]$  interactions. For example, in the crystal structure of **1,3,5-trimethylbenzene@cagearene-1**, one 1,3,5-trimethylbenzene molecule located in the center of the cage cavity forced by strong  $[\pi-\pi]$  stacking with an average distance of 3.6 Å and multivalence of  $[\text{C}-\text{H}\cdots\pi]$  interactions with an average distance of about 3.0 Å. Compared to 8.2 Å of the “roof” to “floor” in the empty cage (Fig. 1a), the corresponding value in **1,3,5-trimethylbenzene@cagearene-1** was decreased to 7.2 Å (Fig. 1c), demonstrating the strong  $[\pi-\pi]$  stacking between 1,3,5-trimethylbenzene and the cage. In the crystal structure of **pentane@cagearene-1**, it was somewhat surprising to us that the cavity of **cagearene-1** was occupied by one pentane molecule, instead of a toluene molecule, which sat outside of the cavity (Fig. 1d). We attribute this phenomenon to the result of multivalence of  $[\text{C}-\text{H}\cdots\pi]$  interactions with an average distance of 3.1 Å between pentane protons and the cage.

### Absorption/separation experiment

In recent years, our group developed a new method to separate hydrocarbon compounds based on pillararenes, and coined the term nonporous adaptive crystals (NACs), where dense packing and guest-free crystalloids were penetrated by preferable guest molecules through solid-vapour contact, and a crystal structure transformation was induced, achieving selective guest separation and adsorption.<sup>18</sup> The proper structural features and the host-guest properties in the solid state of **cagearene-1** provide the essential conditions for its application in the absorption/separation of hydrocarbons.

Benzene (Bz) and cyclohexane (Cy) are both important petrochemical products. However, their separation is challenging by various distillation and purification processes because of their similar physical properties, such as similar sizes (Bz: 4.6 Å and Cy: 4.7 Å in diameter), and close boiling points (Bz: 353.25 K and Cy: 353.85 K).<sup>19</sup> Because Bz and Cy have completely different electrostatic potentials (Fig. 4d), we anticipated that **cagearene-1** might provide a new alternative to separate Bz and Cy.

In order to test its capability for adsorbing Bz or Cy vapour, <sup>1</sup>H NMR and thermogravimetric analysis (TGA) experiments were carried out to investigate the single-component solid-vapour adsorption. It was found that the uptake of Bz was very rapid and almost reached saturation after only 1 h (Fig. 2b and S17†), and eventually reached  $\sim 3$  equivalents of benzene per **cagearene-1** (Fig. S22†). In contrast, the uptake of Cy for **cagearene-1** was saturated after 12 h (Fig. 2b and S18†) and a small amount of cyclohexane (0.6 Cy per **cagearene-1**) was adsorbed in the solid (Fig. S23†). The TGA experiment of **cagearene-1** showed a weight loss of 13.4% at 100 °C after adsorption of Bz vapour for 12 h, confirming that one cage molecule contained about three Bz molecules (Fig. S27†). However, weight loss (3.2%) of **cagearene-1** was relatively slight before 130 °C after adsorption of Cy vapour for 12 h (Fig. S28†). The PXRD spectrum of the activated **cagearene-1** solid after adsorbing Bz showed sharper peaks, suggesting that the amorphous solid had transformed into the crystalline state (Fig. 2a). However, it showed only slight changes after taking up

Cy, indicating that the influence of Cy on molecule packing is slight (Fig. 2a).

Then, the possibility of selectively adsorbing and separating Bz/Cy mixture vapour was verified on activated **cagearene-1** powder. We conducted a time-dependent, solid-vapour sorption experiment for equimolar Bz/Cy mixture vapour (50 : 50 v/v) (Fig. S19†). Like single-component vapour absorption, **cagearene-1** adsorbed Bz more effectively than Cy. It was found that the uptake of Bz reached saturation after only 1 h, and eventually reached  $\sim 3$  equivalents of benzene per **cagearene-1** (Fig. S21†). In contrast, a relatively small amount of cyclohexane (0.4 equivalent Cy per **cagearene-1**) was present in the solid (Fig. S21†). Gas chromatography (GC) experiments showed that the percentage of Bz adsorbed by **cagearene-1** was 91.1% (Fig. S30†).

### Temperature-controlled vapour release

The TGA result of the Bz-adsorbed **cagearene-1** solid showed that the Bz molecules started to release at about 40 °C (Fig. S27†), while in the Cy-adsorbed **cagearene-1** solid, the temperature required to release Cy was about 80 °C (Fig. S28†). We anticipated that the difference of these two desorption temperatures may provide an opportunity to investigate temperature-controlled vapour release. After exposing the **cagearene-1** powder to an equimolar Bz/Cy (50 : 50 v/v) mixture for 12 h, desorption was subsequently conducted at a temperature of 70 °C, which is lower than the desorption temperature at

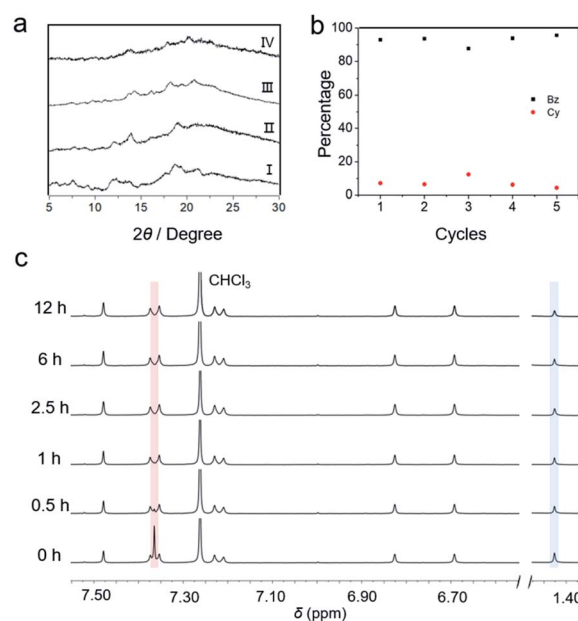


Fig. 3 (a) The PXRD patterns of **cagearene-1**: (I) after adsorption of Bz/Cy equimolar mixture vapour; (II) after desorption of Bz vapour at 70 °C for 12 h; (III) after desorption of Cy at 130 °C for 12 h; (IV) original **cagearene-1**. (b) Relative uptake ratio of Bz and Cy in **cagearene-1** powder through five cycles of activation/adsorption determined by gas chromatography. (c) Time-dependent partial <sup>1</sup>H NMR (400 MHz, 298 K, CDCl<sub>3</sub>) of desorption of Bz/Cy equimolar mixture adsorbed **cagearene-1** at 70 °C (red region: Bz, δ = 7.36 ppm; blue region: Cy, δ = 1.43 ppm).



which Cy absorbed by **cagearene-1**. The  $^1\text{H}$  NMR spectra revealed that the absorbed Bz was desorbed drastically within 30 min, while a small amount of absorbed Cy was removed (Fig. 3c). After 2.5 h, there was no observable proton signal for Bz on the  $^1\text{H}$  NMR scale. In contrast, cyclohexane molecules were present continuously even after 12 h. Upon heating for 12 h at 70 °C, the purity of Cy adsorbed in **cagearene-1** was determined by GC as 98.7% (Fig. S30†). Besides, the PXRD spectrum showed that the resulting **cagearene-1** solid after releasing Bz was transformed into the initial state again (Fig. 3a). Then, the release of Cy was triggered efficiently by exposing the solid at 130 °C overnight.

Cycling performance is an important parameter for evaluating an adsorbent. We demonstrated that the **cagearene-1** powder could separate Bz/Cy mixtures without degradation after recycling five times upon regeneration (Fig. 3b).

### Mechanism analysis of absorption/separation and temperature-controlled vapour release

In order to unravel the underlying mechanism, the detailed structures of the solid with guests were studied by single

crystallography and PXRD analysis. Single crystals of **Bz@cagearene-1** were obtained by directly evaporating a benzene solution of the cage. In the solid state, one **cagearene-1** molecule was surrounded by three Bz molecules, which majorly sat outside of the cage cavity (Fig. 4a and Table S3†). Such a complex formation was driven by [C–H···π] interactions between the guest molecules and cage. However, such interactions were very weak with an average distance of about 4.0 Å. The simulated PXRD spectrum of the **Bz@cagearene-1** crystal also showed a weak signal of the crystalline state (Fig. S31†).

Trials to get single crystals of **Cy@cagearene-1** were unsuccessful. Because Cy has a higher release temperature than Bz, we postulated that Cy has stronger host–guest interactions with **cagearene-1**. In order to verify this hypothesis, computational analysis was performed to study the binding interactions between Cy and **cagearene-1**. A number of binding models were created and optimized, *i.e.*, (a) the guest in the center of the cavity, (b) the guest on the lateral side of the cavity, (c) the guest in the window of the cavity, and (d) the guest outside the cavity (all with the molar ratio of Cy and **cagearene-1** = 1 : 1). Fig. S33† shows the single point energies of the Cy-loaded structures.

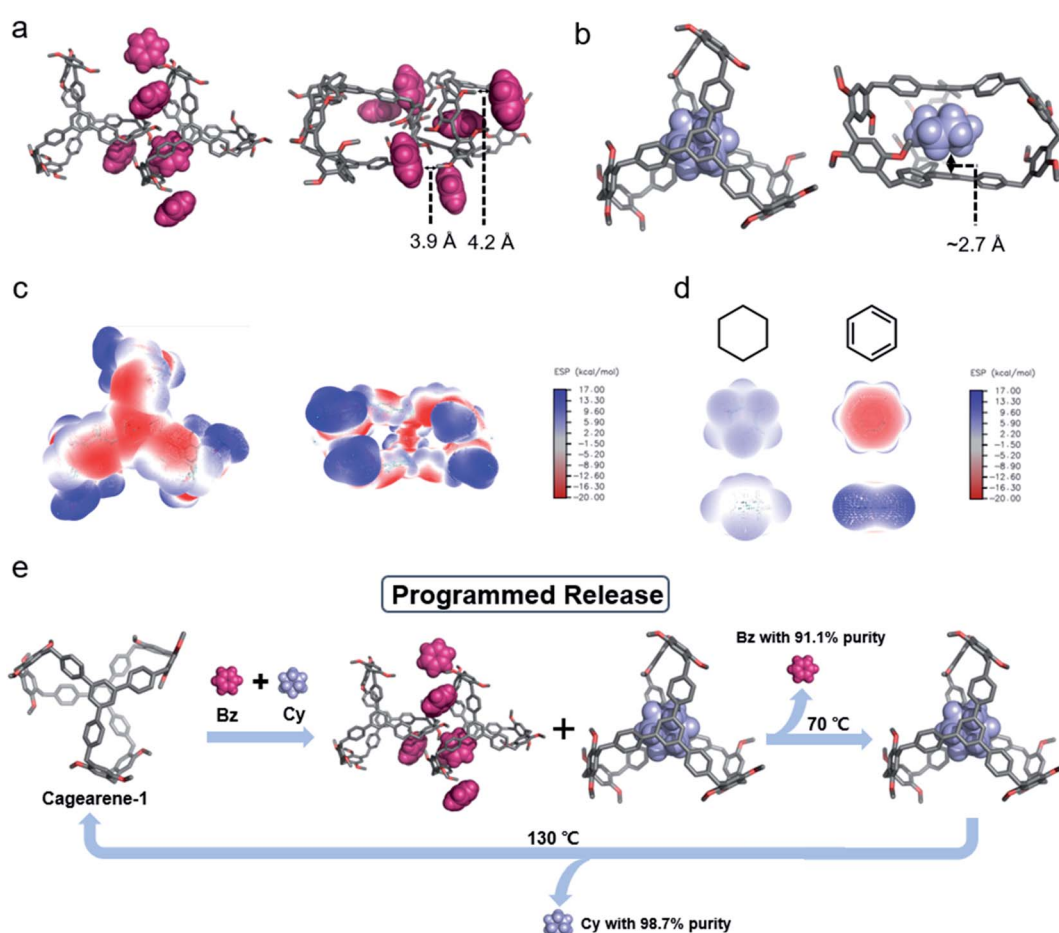


Fig. 4 (a) Single-crystal structure of **Bz@cagearene-1** and (b) optimized structure of **Cy@cagearene-1** with the lowest energy. Electrostatic potential maps: (c) **cagearene-1** (top and side views); (d) Cy and Bz (top and side views). (e) Structural representation of the Bz/Cy fractionation process based on **cagearene-1**. Certain H atoms are omitted for clarity. The guest molecules are illustrated in a space-filling representation, while the cages are illustrated in a stick representation.



These energies suggested that **Cy@cagearene-1**, wherein Cy sat at the center of the cavity, had the lowest energy among the four structures, indicating its stable and preferred formation (Fig. 4b). Upon binding with Cy, the two large phenyl panels on the cage provided sufficient  $\pi$  surface areas to form six  $[\text{C}-\text{H}\cdots\pi]$  interaction sites with an average distance of about 2.7 Å, an ideal position for sandwiching Cy. This preferred structure of **Cy@cagearene-1** was similar to the crystal structure of **pentane@cagearene-1** (Fig. 1d), in which the cavity of **cagearene-1** was occupied by a pentane molecule with multivalence of  $[\text{C}-\text{H}\cdots\pi]$  interactions, instead of a toluene molecule.

Moreover, the electrostatic potential (ESP) map showed that the center of the **cagearene-1** cavity is electronegative and the window of the cavity formed by three lateral edges is electropositive (Fig. 4c). Because the ESP of Cy is electropositive (Fig. 4d), the center of the **cagearene-1** cavity has good stereoelectronic complementarity with a Cy molecule, and provides ideal electrostatic attraction for Cy. Altogether, the  $[\text{C}-\text{H}\cdots\pi]$  interactions and a good stereoelectronic match drive the formation of a stable host-guest complex between Cy and **cagearene-1**.

Combining the single crystal structure and theoretical analyses, the mechanism of selective adsorption/separation and programmed release is summarized as follows: Bz molecules tend to gather at the outside of the cavity of **cagearene-1** quickly in a weak binding manner. However, Cy prefers to form a much more stable host-guest complex with **cagearene-1** forced by multivalence of  $[\text{C}-\text{H}\cdots\pi]$  interactions and electrostatic attraction. When **cagearene-1** is exposed to Bz/Cy mixture vapours, Bz molecules surrounding the cage reach adsorption saturation in a shorter time. This process also prevents further uptake of Cy molecules, affecting the mass transfer of Cy into the cavity. Even so, there is still a small amount of Cy entering the cavity, which prefers to form a more stable host-guest complex with the cage. Then, during desorption, the Bz molecules are released at a lower temperature, while the more strongly bound Cy molecules are desorbed at higher temperatures. Hence, two components with high purities can be obtained separately through temperature-controlled release (Fig. 4e).

## Conclusion

In summary, we successfully developed a new strategy to synthesize molecular cages by taking advantage of the FC reaction. By using different building units, two new cages, namely **cagearene-1** and **cagearene-2**, were synthesized and well characterized. Illustrated by the successful formation of two cages, it was demonstrated that this is a versatile strategy for the construction of diverse cages using different building units. Moreover, the **cagearene-1** solid adsorbs Bz vapour from an equimolar Bz/Cy mixture (50 : 50 v/v) with 91.1% purity. Subsequently through temperature-controlled vapour release, Cy with a purity of 98.7% could be obtained. The cage in the solid state binds Bz molecules in a weak binding manner. In contrast, Cy molecules prefer to form much stronger host-guest interactions with the cage, which is confirmed by theoretical calculations. As a consequence, the adsorbed Bz molecules are

released at a lower temperature, and the Cy molecules are left stable. These results indicate that there are broad prospects for new cage design and fabrication aimed at programmed release for important chemical separations. Such work is now in progress in our laboratory, including (a) using these cages for other applications and (b) synthesis of new cages with various functionalized building blocks, such as tetraphenylethylene (TPE), pyrene, and triphenylamine.

## Data availability

Data for this paper, including synthesis and structural characterization studies, are available in the ESI.†

## Author contributions

Conceptualization: Shuai Fang, Hao Li, and Feihe Huang. Data curation: Shuai Fang, Mengbin Wang, Yating Wu, and Errui Li. Formal analysis: Shuai Fang, Mengbin Wang, Yating Wu, and Errui Li. Investigation: Shuai Fang. Methodology: Shuai Fang, Hao Li, and Feihe Huang. Project administration: Shuai Fang, Hao Li, and Feihe Huang. Resources: Hao Li and Feihe Huang. Software: Shuai Fang. Supervision: Shuai Fang, Mengbin Wang, Errui Li, Hao Li, and Feihe Huang. Validation: Shuai Fang, Mengbin Wang, and Yating Wu. Roles/writing – original draft: Shuai Fang and Errui Li. Writing – review and editing: Qing-Hui Guo, Errui Li, Hao Li, and Feihe Huang.

## Conflicts of interest

There are no conflicts to declare.

## Acknowledgements

F. H. thanks the National Key Research and Development Program of China (2021YFA0910100), the National Natural Science Foundation of China (22035006), the Zhejiang Provincial Natural Science Foundation of China (LD21B020001) and the Starry Night Science Fund of Zhejiang University Shanghai Institute for Advanced Study (SN-ZJU-SIAS-006) for financial support. Hao thanks China State Key Research Grant No. 2016YEF0200503, the Chinese “Thousand Youth Talents Plan”, the National Natural Science Foundation of China (91856116, 21922108 and 21772173), the Natural Science Foundation of Zhejiang Province (No. LR18B02001) and Fundamental Research Funds for the Central Universities (2019FZA3007).

## Notes and references

- (a) S.-H. Kim, H. C. Shum, J. W. Kim, J.-C. Cho and D. A. Weitz, *J. Am. Chem. Soc.*, 2011, **133**, 15165–15171; (b) X. Li, L. Zhou, Y. Wei, A. M. El-Toni, F. Zhang and D. Zhao, *J. Am. Chem. Soc.*, 2014, **136**, 15086–15092; (c) H. Deng, M. A. Olson, J. F. Stoddart and O. M. Yaghi, *Nat. Chem.*, 2010, **2**, 439–443; (d) I. C. Kwon, Y. H. Bae and S. W. Kim, *Nature*, 1991, **354**, 291–293.



2 (a) J. T. Santini, M. J. Cima and R. Langer, *Nature*, 1999, **397**, 335–338; (b) F. Jia, H. V. Schröder, L.-P. Yang, C. von Essen, S. Sobottka, B. Sarkar, K. Rissanen, W. Jiang and C. A. Schalley, *J. Am. Chem. Soc.*, 2020, **142**, 3306–3310.

3 Y. Zhao, B. G. Trewyn, I. I. Slowing and V. S. Y. Lin, *J. Am. Chem. Soc.*, 2009, **131**, 8398–8400.

4 G. Vantomme, S. Jiang and J.-M. Lehn, *J. Am. Chem. Soc.*, 2014, **136**, 9509–9518.

5 (a) Z. Dong, Y. Sun, J. Chu, X. Zhang and H. Deng, *J. Am. Chem. Soc.*, 2017, **139**, 14209–14216; (b) J. An, S. J. Geib and N. L. Rosi, *J. Am. Chem. Soc.*, 2009, **131**, 8376–8377; (c) B. D. Chandler, G. D. Enright, K. A. Udachin, S. Pawsey, J. A. Ripmeester, D. T. Cramb and G. K. H. Shimizu, *Nat. Mater.*, 2008, **7**, 229–235.

6 (a) S. Matsuzaki, T. Arai, K. Ikemoto, Y. Inokuma and M. Fujita, *J. Am. Chem. Soc.*, 2014, **136**, 17899–17901; (b) M. Zhang, X. Yan, F. Huang, Z. Niu and H. W. Gibson, *Acc. Chem. Res.*, 2014, **47**, 1995–2005; (c) L. Isaacs, *Acc. Chem. Res.*, 2014, **47**, 2052–2062; (d) P. Xing and Y. Zhao, *Acc. Chem. Res.*, 2018, **51**, 2324–2334; (e) M. Lee and H. W. Gibson, *Macromolecules*, 2020, **53**, 6747.

7 (a) H. E. Simmons and C. H. Park, *J. Am. Chem. Soc.*, 1968, **90**, 2428; (b) C. H. Park and H. E. Simmons, *J. Am. Chem. Soc.*, 1968, **90**, 2429–2430; (c) C. H. Park and H. E. Simmons, *J. Am. Chem. Soc.*, 1968, **90**, 2431–2432; (d) B. Dietrich, J.-M. Lehn and J.-P. Sauvage, *Tetrahedron Lett.*, 1969, **10**, 2885–2888; (e) B. Dietrich, J.-M. Lehn, J.-P. Sauvage and J. Blanzat, *Tetrahedron*, 1973, **29**, 1629–1645; (f) D. J. Cram, M. E. Tanner and C. B. Knobler, *J. Am. Chem. Soc.*, 1991, **113**, 7717–7727; (g) D. J. Cram, *Nature*, 1992, **356**, 29–36.

8 (a) Y. Shi, K. Cai, H. Xiao, Z. Liu, J. Zhou, D. Shen, Y. Qiu, Q.-H. Guo, C. Stern, M. R. Wasielewski, F. Diederich, W. A. Goddard and J. F. Stoddart, *J. Am. Chem. Soc.*, 2018, **140**, 13835–13842; (b) C. Zhang, Q. Wang, H. Long and W. Zhang, *J. Am. Chem. Soc.*, 2011, **133**, 20995–21001; (c) S. Matsuzaki, T. Arai, K. Ikemoto, Y. Inokuma and M. Fujita, *J. Am. Chem. Soc.*, 2014, **136**, 17899–17901; (d) D. Zhu, S. Fang, L. Tong, Y. Lei, G. Wu, T. Chudhary and H. Li, *Chem. Commun.*, 2021, **57**, 4440–4443; (e) S. Fang, E. Li, D. Zhu, G. Wu, Q. Zhang, C. Lin, F. Huang and H. Li, *Chem. Commun.*, 2021, **57**, 6074–6077.

9 (a) Y. Ni, T. Y. Gopalakrishna, H. Phan, T. Kim, T. S. Herring, Y. Han, T. Tao, J. Ding, D. Kim and J. Wu, *Nat. Chem.*, 2020, **12**, 242–248; (b) J. Zhu, Y. Han, Y. Ni, S. Wu, Q. Zhang, T. Jiao, Z. Li and J. Wu, *J. Am. Chem. Soc.*, 2021, **143**, 14314–14321.

10 (a) M. Liu, L. Zhang, M. A. Little, V. Kapil, M. Ceriotti, S. Yang, L. Ding, D. L. Holden, R. Balderas-Xicohténcatl, D. He, R. Clowes, S. Y. Chong, G. Schütz, L. Chen, M. Hirscher and A. I. Cooper, *Science*, 2019, **366**, 613–620; (b) T. Mitra, K. E. Jelfs, M. Schmidtmann, A. Ahmed, S. Y. Chong, D. J. Adams and A. I. Cooper, *Nat. Chem.*, 2013, **5**, 276–281; (c) B. Moosa, L. O. Alimi, A. Shkurenko, A. Fakim, P. M. Bhatt, G. Zhang, M. Eddaoudi and N. M. Khashab, *Angew. Chem., Int. Ed.*, 2020, **59**, 21367–21371; (d) T. Kunde, E. Nieland, H. V. Schröder, C. A. Schalley and B. M. Schmidt, *Chem. Commun.*, 2020, **56**, 4761–4764.

11 (a) H. Takezawa, K. Shitozawa and M. Fujita, *Nat. Chem.*, 2020, **12**, 574–578; (b) M. Yoshizawa, M. Tamura and M. Fujita, *Science*, 2006, **312**, 251–254; (c) T. Murase, Y. Nishijima and M. Fujita, *J. Am. Chem. Soc.*, 2012, **134**, 162–164; (d) M. R. Crawley, D. Zhang, A. N. Oldacre, C. M. Beavers, A. E. Friedman and T. R. Cook, *J. Am. Chem. Soc.*, 2021, **143**, 1098–1106.

12 (a) R. McCaffrey, H. Long, Y. Jin, A. Sanders, W. Park and W. Zhang, *J. Am. Chem. Soc.*, 2014, **136**, 1782–1785; (b) Q. Zhu, X. Wang, R. Clowes, P. Cui, L. Chen, M. A. Little and A. I. Cooper, *J. Am. Chem. Soc.*, 2020, **142**, 16842–16848; (c) W. Liu, S. K. Samanta, B. D. Smith and L. Isaacs, *Chem. Soc. Rev.*, 2017, **46**, 2391–2403; (d) M. Kohlhaas, M. Zähres, C. Mayer, M. Engeser, C. Merten and J. Niemeyer, *Chem. Commun.*, 2019, **55**, 3298–3301; (e) S. Pullen, J. Tessarolo and G. H. Clever, *Chem. Sci.*, 2021, **12**, 7269–7293; (f) T. R. Schulte, J. J. Holstein, L. Schneider, A. Adam, G. Haberhauer and G. H. Clever, *Angew. Chem., Int. Ed.*, 2020, **59**, 22489–22493; (g) K. Wu, B. Zhang, C. Drechsler, J. J. Holstein and G. H. Clever, *Angew. Chem., Int. Ed.*, 2021, **60**, 6403–6407; (h) U. Warzok, M. Marianski, W. Hoffmann, L. Turunen, K. Rissanen, K. Pagel and C. A. Schalley, *Chem. Sci.*, 2018, **9**, 8343–8351.

13 (a) S. J. Rowan, S. J. Cantrill, G. R. L. Cousins, J. K. M. Sanders and J. F. Stoddart, *Angew. Chem., Int. Ed.*, 2002, **41**, 898–952; (b) Y. Jin, C. Yu, R. J. Denman and W. Zhang, *Chem. Soc. Rev.*, 2013, **42**, 6634–6654; (c) G. Zhang and M. Mastalerz, *Chem. Soc. Rev.*, 2014, **43**, 1934–1947; (d) N. M. Rue, J. Sun and R. Warmuth, *Isr. J. Chem.*, 2011, **51**, 743–768; (e) K. Acharyya and P. S. Mukherjee, *Angew. Chem., Int. Ed.*, 2019, **58**, 8640–8653.

14 (a) E. J. Dale, N. A. Vermeulen, M. Juriček, J. C. Barnes, R. M. Young, M. R. Wasielewski and J. F. Stoddart, *Acc. Chem. Res.*, 2016, **49**, 262–273; (b) B. M. Rambo, H.-Y. Gong, M. Oh and J. L. Sessler, *Acc. Chem. Res.*, 2012, **45**, 1390–1401; (c) X. Chi, W. Cen, J. A. Queenan, L. Long, V. M. Lynch, N. M. Khashab and J. L. Sessler, *J. Am. Chem. Soc.*, 2019, **141**, 6468–6472.

15 X. Zhao, Y. Liu, Z.-Y. Zhang, Y. Wang, X. Jia and C. Li, *Angew. Chem., Int. Ed.*, 2021, **60**, 17904–17909.

16 (a) M. Fujita, D. Oguro, M. Miyazawa, H. Oka, K. Yamaguchi and K. Ogura, *Nature*, 1995, **378**, 469–471; (b) N. Hafezi, J. M. Holcroft, K. J. Hartlieb, E. J. Dale, N. A. Vermeulen, C. L. Stern, A. A. Sarjeant and J. F. Stoddart, *Angew. Chem., Int. Ed.*, 2015, **54**, 456–461.

17 C. Zhang, H. Wang, J. Zhong, Y. Lei, R. Du, Y. Zhang, L. Shen, T. Jiao, Y. Zhu, H. Zhu, H. Li and H. Li, *Sci. Adv.*, 2019, **5**, eaax6707.

18 (a) K. Jie, Y. Zhou, E. Li and F. Huang, *Acc. Chem. Res.*, 2018, **51**, 2064–2072; (b) E. Li, K. Jie, Y. Zhou, R. Zhao and F. Huang, *J. Am. Chem. Soc.*, 2018, **140**, 15070–15079; (c) M. Wang, J. Zhou, E. Li, Y. Zhou, Q. Li and F. Huang, *J. Am. Chem. Soc.*, 2019, **141**, 17102–17106; (d) E. Li, K. Jie, Y. Fang, P. Cai and F. Huang, *J. Am. Chem. Soc.*, 2020, **142**, 15560–15568; (e) J.-R. Wu, B. Li and Y.-W. Yang, *Angew. Chem., Int. Ed.*, 2020, **59**, 2251–2255; (f) Y. Wu, J. Zhou, E. Li, M. Wang, K. Jie, H. Zhu and F. Huang, *J. Am. Chem.*



*Soc.*, 2020, **142**, 19722–19730; (g) Q. Li, K. Jie and F. Huang, *Angew. Chem., Int. Ed.*, 2020, **59**, 5355–5358; (h) X. Sheng, E. Li, Y. Zhou, R. Zhao, W. Zhu and F. Huang, *J. Am. Chem. Soc.*, 2020, **142**, 6360–6364; (i) Y. Wang, K. Xu, B. Li, L. Cui, J. Li, X. Jia, H. Zhao, J. Fang and C. Li, *Angew. Chem., Int. Ed.*, 2019, **58**, 10281–10284.

19 (a) J. Zhou, G. Yu, Q. Li, M. Wang and F. Huang, *J. Am. Chem. Soc.*, 2020, **142**, 2228–2232; (b) W. Yang, K. Samanta, X. Wan, T. U. Thikekar, Y. Chao, S. Li, K. Du, J. Xu, Y. Gao, H. Zuilhof and A. C.-H. Sue, *Angew. Chem., Int. Ed.*, 2020, **59**, 3994–3999; (c) H. Yao, Y.-M. Wang, M. Quan, M. U. Farooq, L.-P. Yang and W. Jiang, *Angew. Chem., Int. Ed.*, 2020, **59**, 19945–19950; (d) Y. Ding, L. O. Alimi, B. Moosa, C. Maaliki, J. Jacquemin, F. Huang and N. M. Khashab, *Chem. Sci.*, 2021, **12**, 5315–5318.

